General Disclaimer

One or more of the Following Statements may affect this Document

- This document has been reproduced from the best copy furnished by the organizational source. It is being released in the interest of making available as much information as possible.

- This document may contain data, which exceeds the sheet parameters. It was furnished in this condition by the organizational source and is the best copy available.

- This document may contain tone-on-tone or color graphs, charts and/or pictures, which have been reproduced in black and white.

- This document is paginated as submitted by the original source.

- Portions of this document are not fully legible due to the historical nature of some of the material. However, it is the best reproduction available from the original submission.

N O T I C E

THIS DOCUMENT HAS BEEN REPRODUCED FROM MICROFICHE. ALTHOUGH IT IS RECOGNIZED THAT CERTAIN PORTIONS ARE ILLEGIBLE, IT IS BEING RELEASED IN THE INTEREST OF MAKING AVAILABLE AS MUCH INFORMATION AS POSSIBLE
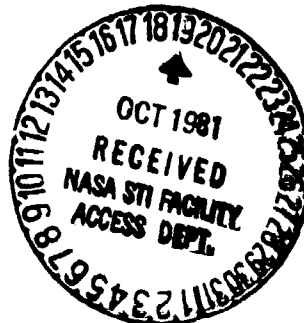
CELL MODULE AND FUEL CONDITIONER

7TH QUARTERLY REPORT: APRIL-JUNE, 1981

D.Q. Hoover, Jr.
Westinghouse R&D Center
Westinghouse Electric Corporation
Pittsburgh, PA. 15235

July, 1981

OCT 1981
RECEIVED
NASA STI FACILITY
ACCESS DEPT.

CELL MODULE & FUEL CONDITIONER DEVELOPMENT

7TH QUARTERLY REPORT: APRIL-JUNE, 1981

D.Q. Hoover, Jr.
Westinghouse R&D Center
Westinghouse Electric Corporation

July, 1981

TABLE OF CONTENTS

Page

I. INTRODUCTION

This report is for the second Phase of a six Phase program to develop commercially viable on-site integrated energy systems (OS/IES) using phosphoric acid fuel cell (PAFC) modules to convert fuel to electricity. Phase II is a planned two year effort to develop appropriate fuel cell module and fuel conditioner conceptual designs. The fuel cell module development effort comprises three coordinated tasks:

Task 1: Design of Large Cell Stacks

Task 2: Stack Fabrication

Task 3: Stack Testing

The "Fuel Conditioner Subsystem Development" task is the fourth technical task of this effort. Provision for "Management, Reporting and Documentation" is included as a fifth task.

The work accomplished during this reporting period is described at the subtask level in the following section.

II. TECHNICAL PROGRESS

TASK 1: DESIGN OF LARGE CELL STACKS

1.2 Stack Design

Stack 564 (23 cell, MK-2)

Stack 564 is similar to Stack 562 which was described in previous reports and in a procedures document submitted to the NASA Project Manager separately. The differences include a refinement of the cooling channel design and a support for the matrix over the acid reservoir.

Figure 1 is the drawing of the cooling plate halves machined for Stack 564. Analysis of the thermal data obtained during the testing of Stack 562 indicated that this design will result in more uniform temperature distributions in the stack.

Post-test analysis of Stack 561* indicated that support of the matrix over the acid reservoir would improve acid management by preventing intrusion of the matrix into the reservoir.

Five Cell Modules

Preassembly of five cell modules may aid in assembly and repair of long stacks. To test this concept, four modules (two for each design) are being designed. Each module will consist of five cells (standard electrochemical components and heat-treated graphite/resin plates) and one cooling half-plate on each end. The design of the mechanism for holding the modules together is being developed.

Stack 800 (80 cell, MK-2)

Due to schedular and funding limitations, the assembly scheme and hardware for Stack 800 will be basically the same as that of previous

---

* Refer to Sub task 3.3   Short Stack Testing
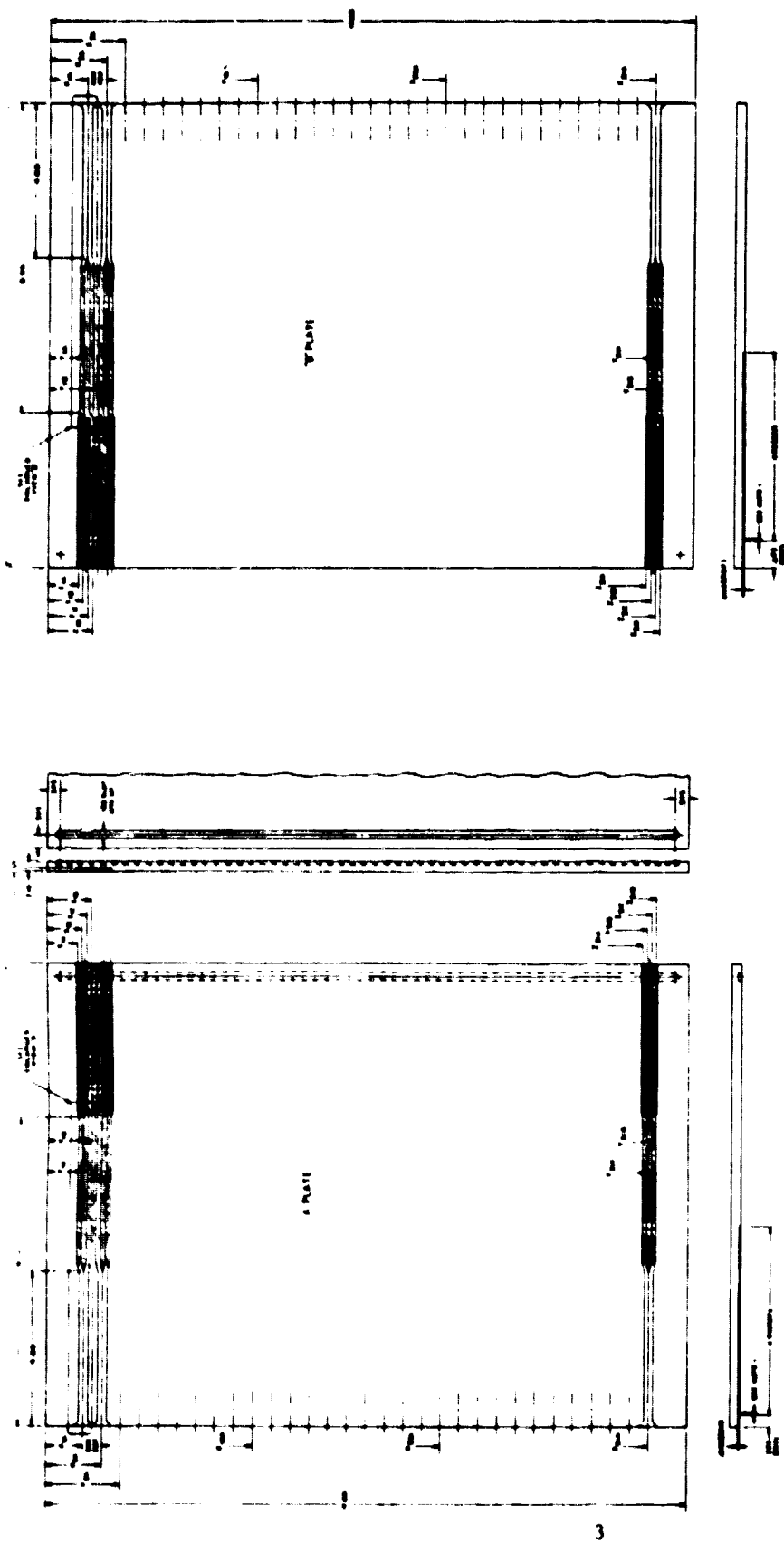
2

Figure 1 - Cooling Plate Design for Stack 564

stacks. A fabrication procedures document describing the design and construction of this stack will be prepared and forwarded to the NASA Project Manager.

TASK 2: STACK FABRICATION

2.1 Methods and Approach

Five Cell Modules

M65 and M67 (5 cell, MK-1 modules)

The cooling/end plates for M65 and M67 were molded and leak-tested during April and delivered for machining. The molding of the bipolar plates for these modules was completed during May. The electrodes and matrices have been fabricated and assembly of the modules can take place 3-4 weeks after the machined plates are returned from the machining vendor. We expect to receive these plates during the first part of July.

M66 and M68 (5 cell, MK-2 modules)

The flat plates for M66 and M68 (five cell modules of MK-2 design) were molded and leak-tested during April and sent for machining which is scheduled to be completed during the first part of July. Module assembly will take place about one month after the machined plates are returned.

2.2 Simulated Stack Fabrication

None was scheduled for this quarter.

2.3 Short Stack Fabrication

Stack 563 (23-cell, MK-1)

The bipolar and cooling/end plates for Stack 563 were heat-treated and leak-tested. During deflashing of the center plates, it was found that the edges of the plates along the ~30 cm direction were soft. Investigation of this problem, indicated that the heat-treatment

cycle had not caused the soft spots because other plates (molded both with Varcum and Colloid resins) from the same heat-treatment batch did not have similar defects. Our production records showed that all of the defective plates were molded with one resin batch from a new drum received from the manufacturer. Discussion with the manufacturer indicated that the resin might have advanced in storage. Fabrication of Stack 563 was canceled after discussions with the NASA Project Manager.

Stack 564 (23-cell, MK-2)

The molding and leak-testing of all plates for this stack was completed in April and plates were sent out for machining. Fabrication of electrodes and matrices was completed. Stack assembly will take place 4 - 6 weeks after the machined plates are returned by the vendor.

2.5 Subscale Stack Fabrication

Stack 800 (80 cell, MK-2)

Approval was received during this quarter to begin fabrication of the first subscale (80 cell) stack of MK-2 design. Molding of the thick cooling/end plates was completed by June 19. After molding of the other plates is completed, the batch of plates will be sent for machining.

TASK 3: STACK TESTING

3.1 OS/IES Loop Modifications

The modifications made on the OS/IES Simulation Loop provide for:

1. Automatic acquisition and recording of data.
2. Operation at selectable constant current.
3. Safe unattended operation of the loop.

The major items of equipment installed under this contract to achieve these functions are a Fluke Data Logger, a constant current power supply and a signal line to the continuously manned security station.

The data logger provides 30 alarm outputs in addition to its 1000 channel monitoring and recording capability. The 30 alarm channels are used to monitor:

1. Lower limits on individual cell voltages.
2. Upper and lower limits on current.
3. Upper limits on several cell thermocouples.
4. Upper and lower limits on the temperatures of the air and fuel supplies to the fuel cell stack.

When any of these limits are exceeded, the following automatic shutdown sequence is implemented:

1. The constant current power supply is shut down by a relay in its 440 VAC line.
2. A contactor opens removing load from the stack.
3. The fuel supply is shut off and a nitrogen purge of the fuel loop is turned on by a 3-way solenoid valve.
4. Power to the loop air heater is shut-off.
5. The alarm in the security station is activated. Recovery from this sequence requires manual reset by operating personnel.

A system which continuously monitors hydrogen concentration in the hood enclosing the loop, in the hood ventilation duct and in the test room also activates the alarm in the security station if any hydrogen is detected. If the detected hydrogen levels approach a second (higher) selected level, the automatic shut down sequence described above is implemented.

A backup safety system is provided by a comparative digital voltmeter which monitors the stack voltage and initiates the shutdown sequence if the high or low set points are exceeded. This protects against a wide range of system failures such as loss of fuel or process air, loss of load, failure of the loop heaters, etc., which will cause the stack voltage to exceed the selected limits.

3.2 Simulated Stack Testing

Stack 560 (5-cell, MK-2)

Endurance testing of Stack 560 continued this quarter. Figure 2 is an updated lifegraph showing the 3600 hours of operation accumulated thus far. The time-averaged performance of Stack 560 is 613 mV per cell at 150 mA/cm^2 with hydrogen. Individual cell performance after 3200 hours of operation is presented in Table I. The air flow rate to the stack was increased from 2.5 to ∿3.0 stoichs (42 lpm) due to slight air sensitivity of the stack.

TABLE I - PERFORMANCE OF STACK 560 (AT 177°C) AFTER 3200 HRS.

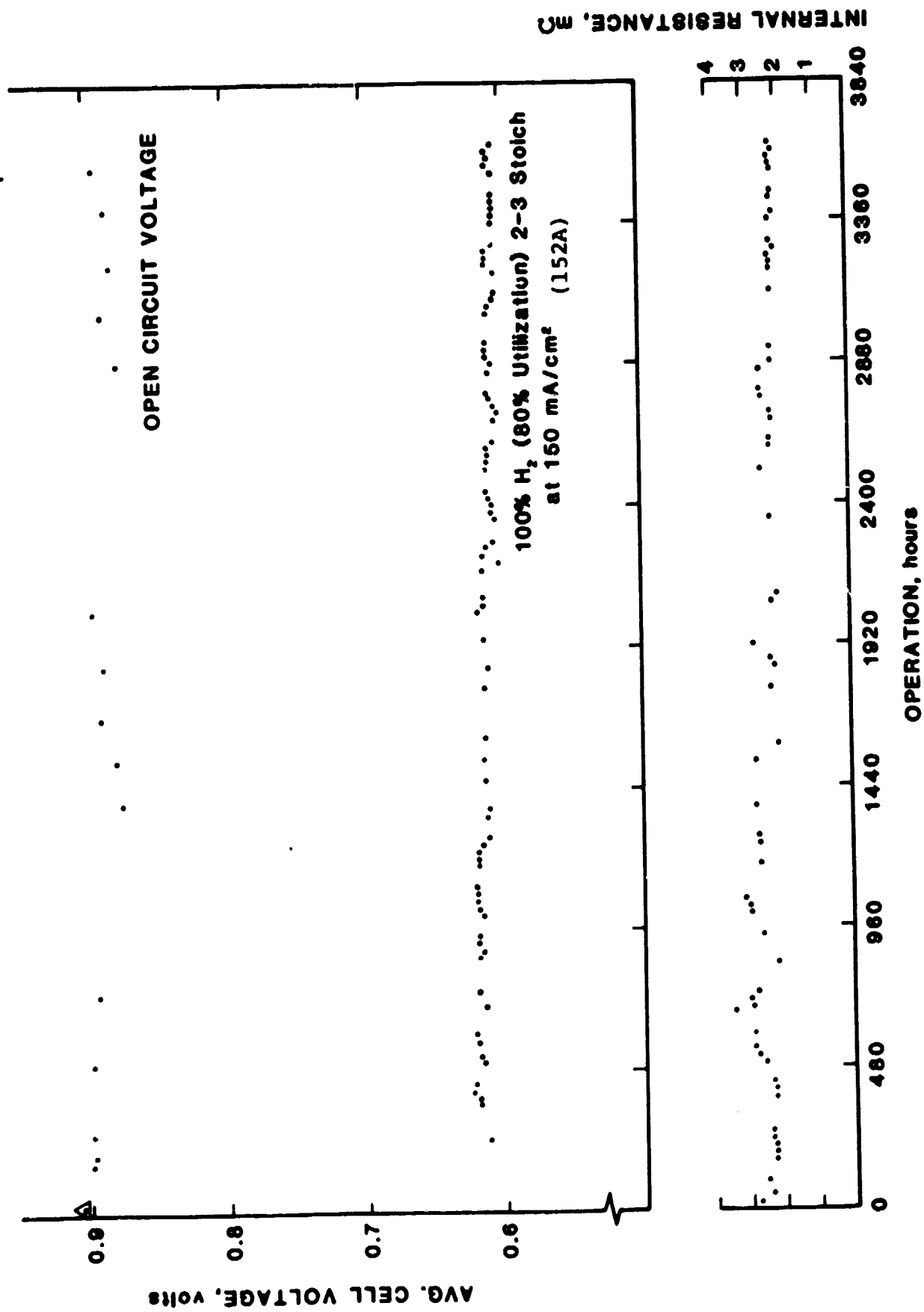| PARAMETERS	PERFORMANCE VOLTS/CELL @ 150 mA/cm^2 (152 A)	OCV H$_2$, AIR
Cell No. 1	0.619	0.836
Cell No. 2	0.585	0.918
Cell No. 3	0.595	0.894
Cell No. 4	0.638	0.898
Cell No. 5	0.615	0.873
Average Cell Voltage	0.610	0.884
Fuel	100% H$_2$ Humidified at R.T.	
Fuel Flow	7.3 SLM	
H$_2$ Utilization	81%	
Air Flow	42 SLM ∿ 3.0 Stoichs	

FIGURE 2 – LIFE GRAPH OF STACK 560

8

3.3 Short Stack Testing

Stack 562 (23-cell, MK-2)

During this reporting period the OS/IES loop testing of Stack 562 was completed.

The objectives of these tests were:

1. Verify the ability of the treed cooling channels to achieve cell temperature differentials substantially smaller than the cooling gas temperature rise over a wide range of operating conditions.

2. Acquire data on the effects of various operating parameters (e.g., fuel utilization, temperature level, fuel CO content) on cell performance, temperature distribution and pressure drops for verification and/or modification of the equations used in the lumped parameter and detailed analytical model computer programs.

In accordance with the above objectives, Stack 562 was operated at 131 steady state conditions (including 29 tests in the prior period) which are described, along with the results and discussion, below.

Stack 562 is a 23-cell MK-2 (Z bipolar plate) stack with four treed cooling plates located after cells 4, 9, 14 and 19. The Z channel stack provides for separate cooling gas and process air flows. The stack includes heat treated bipolar and cooling plates and Mat-1 matrices. The active area after heat treatment is approximately 1030 cm^2. Each cooling plate has 31 equally spaced treed channels of the same design as stack 561. Cooling air enters and exits perpendicular to the 43.2 cm face of the stack. The 30.5 cm faces are manifolded in two equal sections with opposite faces each containing a process air and a fuel inlet/outlet manifold. For the normal flow direction, the process air and fuel inlets are near the cooling air inlet edge of the stack. For the reverse flow direction, the flow direction of fuel and process streams are reversed.

9

Tables II and III present a summary of test results and
conditions for Stack 562. Results of the first 29 tests in Table II
were described in the 6th Quarterly Report. Tests 30 through 45 were
made to obtain a performance map as a function of average cell tempera-
ture (150 to 180°C) and current density (50 to 200 mA/cm^2). Tests 46
through 92 were made to determine the effect of CO on performance. Tests
93 through 102 were made to determine the effect of reversed process
flow directions on performance and temperature distribution. Tests 103
through 127 included various combinations of fuel and process air inlet
temperatures as well as different cooling temperature rises to obtain
the effects of these variables on the temperature distribution. Test
128 was run at the maximum current capability of the test loop
(253 mA/cm^2). For test 129 the process flow was changed back to the
normal direction and the stack was tested at the same conditions as
test 110 to verify that stack performance was unchanged. Tests 105
through 131 were made without CO_2 added to the fuel to maintain acceptable
performance of cells 1 and 12 which were more sensitive to hydrogen flow
and concentration than the other cells. An attempt was made to correct
this by cleaning acid from the process channels with very high gas
flow. Test 130 and 131 had the same test conditions as 129 (and 110)
and were made following these efforts. The data indicated that no
significant improvement was made.

Performance of stack 562 was stable during the first 90 tests
with a loss of less than 10 mV per cell. Cell No. 12 showed weak
performance, about 50 mV below average at 150 mA/cm^2, during the
entire test period. When process flow directions were reversed (test 95),
cell No. 1 became weaker than cell 12 and remained the poorest cell
for the rest of the tests.

Effect of Temperature on Performance

Figure 3 shows the performance of Stack 562 for 4 and 2 stoichs
of process air as a function of average temperature. Performance at 2

10

TABLE II – SUMMARY OF TEST CONDITIONS AND TEST RESULTS FOR STACK 562

Test	Current Density mA/cm²	Volts/Cell V	Average Temperature °C	Peak to Average Gradient °C	Fuel Utilization	Dry H₂ Inlet Mole Fraction	Fuel Inlet Temperature °C	Process Air Stoichs	Process Air Inlet Temperature °C	Cooling Air Flow g/sec	Cooling Air Inlet Temperature °C	Cooling Air Temperature Rise °C	Process Air Pressure Drop in.H₂O	Cooling Air Pressure Drop in.H₂O
1	144	.613	173	11.3	.77	.76	114	2.1	123	2.5×10	122	38	3.70	1.73
2	146	.612	168	15.1	.80	.75	128	3.7	124	4.81×10	125	36	–	–
3	146	.614	171	13.1	.80	.75	125	3.7	135	3.4×10	124	39	–	–
4	146	.610	170	10.2	.60	.75	125	3.7	162	3.4×10	123	38	–	2.25
5	150	.585	170	18.4	.82	.75	126	2.0	160	3.7×10	109	52	–	2.25
6	150	.586	173	15.4	.82	.75	133	2.0	183	3.7×10	109	54	–	2.25
7	150	.586	173	15.4	.82	.75	133	2.0	187	3.7×10	109	54	–	2.26
8	150	.599	174	8.1	.72	.75	136	2.0	192	3.7×10	108	54	–	2.26
9	150	.601	173	9.7	.61	.75	139	2.0	175	3.86×10	108	54	3.35	2.29
10	150	.596	171	7.0	.71	.75	138	2.0	190	3.90×10	109	53	3.35	2.30
11	150	.607	172	8.4	.71	.75	135	3.0	150	3.90×10	114	50	4.74	2.30
12	150	.609	171	9.5	.71	.72	137	4.0	151	3.90×10	114	44	4.64	2.30
13	150	.601	175	7.1	.71	.75	135	2.2	148	3.90×10	114	51	3.20	2.30
14	150	.589	151	11.0	.70	.75	143	4.0	128	3.86×10	92	53	6.05	2.23
15	150	.598	156	11.5	.70	.75	141	4.0	128	3.81×10	98	44	6.10	2.24
16	150	.603	163	10.0	.70	.75	142	4.0	140	3.76×10	105	50	6.16	2.24
17	150	.610	175	9.4	.70	.75	147	4.0	154	3.76×10	118	48	6.28	2.26
18	100	.628	153	6.9	.71	.75	134	3.9	142	2.4×10	98	51	3.86	1.11
19	100	.632	158	7.1	.71	.75	134	3.9	148	2.4×10	105	50	3.89	1.12
20	100	.641	169	7.1	.71	.75	136	4.0	159	2.4×10	117	48	3.99	1.14
21	100	.648	179	7.6	.71	.75	137	3.9	166	2.4×10	128	47	4.10	1.17
22	200	.560	160	8.8	.71	.75	148	4.0	156	5.33×10	87	55	8.20	3.44
23	200	.558	166	10.1	.71	.75	151	3.9	156	5.29×10	96	54	8.20	3.44
24	200	.573	174	10.0	.71	.75	151	3.9	163	5.29×10	105	54	8.32	3.44
25	200	.547	151	11.3	.71	.75	149	3.9	139	5.61×10	78	56	7.97	3.99
26	50	.674	151	6.8	.71	.75	116	4.0	140	1.1×10	103	48	1.84	.40
27	50	.681	161	7.0	.71	.75	132	4.0	146	1.0×10	118	42	1.91	.39
28	50	.688	170	7.1	.71	.75	134	4.0	154	1.1×10	130	39	1.95	.40
29	50	.694	179	6.8	.71	.75	136	3.9	162	1.1×10	141	36	1.99	.41

11

TABLE III - SUMMARY OF TEST CONDITIONS AND TEST RESULTS FOR STACK 562

TABLE III - SUMMARY OF TEST CONDITIONS AND TEST RESULTS FOR STACK 562 (continued)

Test	Current Density, mA/cm²	Average Volts/Cell	Average Temperature, °C	Peak to Average Gradient, °C	Fuel Utilization	Dry H₂ Inlet Mole Fraction	Dry CO Inlet Mole Fraction	Fuel Inlet Temperature, °C	Process Air Stoichs	Process Air Inlet Temperature, °C	Cooling Air Flow, g/sec	Cooling Air Inlet Temperature, °C	Cooling Air Temperature Rise, °C	Process Air Pressure Drop, in H₂O	Cooling Air Pressure Drop, in H₂O	Mole Fraction of H₂O in Fuel Exhaust	Fraction of Produced Water Transferred to Fuel

TABLE III – SUMMARY OF TEST CONDITIONS AND TEST RESULTS FOR STACK 562 (continued)

Dwg. 5997C30

TABLE III – SUMMARY OF TEST CONDITIONS AND TEST RESULTS FOR STACK 562 (CONTINUED)

Test	Current Density mA/cm²	Average volts/Cell	Average Temperature, °C	Peak to Average Gradient, °C	Fuel Utilization	Dry H₂ Inlet Mole Fraction	Dry CO Inlet Mole Fraction	Fuel Inlet Temperature, °C	Process Air, Stoichs	Process Air Inlet Temperature, °C	Cooling Air flow, g/sec	Cooling Air Inlet Temperature, °C	Cooling Air Temperature Rise, °C	Process Air Pressure Drop, in H₂O	Cooling Air Pressure Drop, in H₂O	Mole Fraction of H₂O in Fuel Exhaust	Fraction of Produced Water Transferred To Fuel

Figure 3 - Performance of Stack 562 as a Function of
Temperature for 2 and 4 Stoich Process Air

stoichs ranged from 10 to 16 mV lower than for 4 stoich. The temperature sensitivity ranges from .67 mV/°C at 50 mA/cm^2 to 1.09 mV/°C at 200 mA/cm^2.

Effect of CO on Performance

Forty-nine quasi-steady tests were run to determine the effect of CO on performance. These tests are termed quasi-steady since only 20 minutes was allowed at each test condition when changing CO level. Dry CO mole fractions in the fuel ranged from 0 to 4.8 percent. The voltage loss was proportional to inlet mole fraction of CO at each test condition. According to the theoretical model the CO effect doubles for every 15°C drop in temperature. Thus,

$$\Delta V \ (T) = \Delta V(177) \times 2^{\left(\frac{177-T}{15}\right)}$$

can be used to correct CO effect measured at T to a reference of 177°C. This relation appeared to be satisfied reasonably well and was used to correct data to a reference temperature of 177°C. Table IV gives the CO effect at 177°C expressed in mV/(percent CO in the inlet fuel). The CO effect increases approximately linearly with current density up to 150 mA/cm^2 but the value at 200 mA/cm^2 is about 35 percent higher than predicted by a linear fit of the lower current density data.

Temperature Uniformity

The temperature distribution in Stack 562 was discussed in detail in the 6th Quarterly Report for a nominal 55°C cooling air temperature rise. Results for other flows and inlet temperatures are described in the following paragraphs.

The effects of varying fuel inlet temperature from 77-169°C and process air inlet temperature from 90-166°C were measured for the standard current density (150 mA/cm^2), cooling air inlet temperature (110°C), and cooling air temperature rise (55°C). With one exception, the peak to average cell temperature differences were between 5 and 11°C which are .09 to .20 times the cooling air temperature rise. With a very low process air temperature (91°C) and a very high fuel temperature (163°C) the difference was 13°C or 0.24 times cooling air rise.

16

TABLE IV - EFFECT OF CO ON VOLTAGE AT
TEST CURRENT DENSITIES

Current Density mA/cm^2	CO effect at 177°C mV/(%CO)
50	.9
100	2.1
150	2.8
200	5.1

For a current density of 253 mA/cm^2, the peak to average difference was 9.1°C or .18 times the cooling air temperature rise of 52°C.

The cooling air temperature rise (which is inversely proportional to cooling air flow rate) was varied from 36°C to 82°C for a current density of 150 mA/cm^2 with an average cell temperature of about 170°C. The peak to average differences varied between 5.5 and 10.2°C but, due to the complexity of the pattern changes and small changes in other operating parameters, did not easily correlate to cooling air rise.

Spent Fuel Dew Point

Measurements of spent fuel dew points to determine the portion of the generated water vapor that is carried out by this stream were made for 39 tests and the results are given as mole fraction of the stream and portion transferred in Table III. For 15 tests (most with reversed flow) with 2 stoichs process air and 71% utilization of a fuel stream consisting of room temperature humidified hydrogen, an average 4.4% of the generated water vapor was carried out in the spent fuel stream. For 3 tests with normal flow and ∿62% utilization of a fuel of 75% H_2 - 25% CO_2 on dry basis and 2 stoichs process air this increased to approximately 11%.

The results indicate that:

1. Increasing makeup air flow decreases the water vapor transfer as one would expect since the driving force (partial pressure on the air side) is reduced.

2. The addition of CO to the fuel increases the amount of water vapor transferred (e.g., tests 61 and 62 and 68 and 69).

Stack 561 (23-cell, MK-1)

Post-test analysis of the cell components of Stack 561 was performed. Overall, the electrochemical components of the cells appeared

18

to be on the dry side. Very little blockage of process channels (anode or cathode) was observed. Both current collectors were dry and in good condition. However, one bipolar plate, between Cells 18 and 19, had a hairline crack in the air out/fuel out corner which explains the lower performance of these cells. In addition, in several cells the unsupported matrices had collapsed into the acid reservoirs obstructing acid flow. This indicates the necessity of employing either a matrix support in the channel area or a new channel design.

2 kW Test Facility

During this quarter the following work was completed:

- The programming of the computer for data acquisition was completed and the automatic data acquisition system is now ready for use.

- An additional cooling coil was added to the sample conditioning assemblies of the oxygen analyzers to remove water and lessen the frequency at which the dessicant in the sampling line must be changed.

- The moisture analyzer was repositioned in a cooler zone in the loop exhaust air since it was too hot (above 200°F) to function properly in its original location.

- All thermocouples were checked, marked and bundled to reduce set up time when stack testing begins.

Acid Feed

During the OS/IES loop testing of stack 562, 260 cc of acid were fed through the fill tube at the top of the stack with no clear evidence of acid flow from the exit tube at the bottom of the stack. The cells did not exhibit any symptoms of a serious shortage or excess of acid. The added acid could be accounted for by filling of the reservoirs in the plates and an additional 7 cc of wetted volume in the matrices and/or electrodes.

With a head of about 3.7 cm of acid in the tube the flow rate into the stack is about 1 cc/hr. It appears that the inlet flow is limited by the very high viscosity of the acid in the fill tube and its reservoir which are essentially at room temperature.

Stack Compression

The strain gauges on the compression rods indicate that the stack compression decreased about 24% (from 345 to 262 kPa) since it was assembled. This is apparently due to the permanent deformation of the cell and shim materials described in previous reports and does not impair cell resistances or edge sealing.

3.4 8 kW Test Facility

The ERC 8 kW test facility construction was completed during this quarter. Specific work was:

- The power relays to activate the safety system hydrogen shut-off valve and CO_2 purge valve if a power failure and/or a hydrogen leak occur in the system were installed.

- The humidifier heater controls were installed.

- The thermocouple connections from the loop to the terminal strip were made.

- The MK-2 process air and hydrogen flow meters were calibrated.

- Several dry runs were made to check out each component as well as sections of the loop.

The test station is now ready to receive a stack for manual operation. Programming for data logging has been initiated and will be completed before the 8 kW stack is fabricated.

TASK 4: FUEL CONDITIONER DEVELOPMENT

4.1 Fuel and Water Definitions

This subtask is essentially complete. No work was planned or done during this quarter.

4.2 Operational Requirements

A; designed and quoted on by American Standard and Harrison Div. of G.M., the hot air side of the boiler (B-1 in Figure 4) has a gas side pressure drop of less than 2.5 cm H_2O. This is considerably lower than the value specified for B-1 and assumed in specifying the recycle compressor.

As reported in the 6th Quarterly Report, a significant portion of the water vapor generated in the fuel cell migrates to the anode gas and is carried out in the spent fuel stream. To recover this water the fuel condenser (CD-2 in Figure 4) would have to be located downstream of the fuel cell (in the spent fuel stream) However, measurements on Stack 562 (a MK-2 stack) indicate that the amount of water migrating to the anode gas is too small to justify relocation of CD-2.

4.3 Catalyst Data Base

This subtask is essentially complete. No work was planned or done during this quarter.

4.4 Ancillary Subsystem Data Base

Burner Development

The b urner fuel combustion, fuel/air preheat, and turndown tests were completed in March and reported in the 6th Quarterly Report. Work began on tests of the heat exchange section fabricated as part of the combustion outlet duct during this quarter. These tests were planned

21

Figure 4

22

to provide packed bed heat transfer data to resolve the disparities
in calculations based on published correlations (Table XII of the 2nd
Quarterly Report). The basis for those correlations was investigated
in several references, and is summarized as a Nusselt versus Reynolds
number plot in Figure 5. A conservative selection of Leva's correlation
for the design of the reformer would lead to a slightly oversized reformer.
This selection would allow for a test cell to be fabricated which would
allow for a wide range of test conditions to be investigated without
critical loss of data at the slower reforming conditions. Thus, the Leva's
correlation was incorporated in the computer model discussed in Subtask 4.8
and used in sizing the 10 kW reformer.

Using the computer model with the Leva's correlation to predict
the performance of UTC's 40 kW reformer configuration provided a heat
transfer coefficient and a resultant hydrogen production in the reformer
too low for the production of 40 kW in the fuel cells. This indicated
that (assuming the same catalyst activity was used) UTC had based their
design on a heat transfer correlation less conservative than the Leva
correlation.

As indicated in Figure 6, a 44 mm (1.75 inch) by 152 mm (6.00 inch)
rectangular cross section heat exchanger was installed downstream of the re-
former burner test rig previously used for the determination of the lean
flammability limits of the spent anode gas. This section is packed with 12 mm
(0.5 inch) diameter stainless steel balls. With a fuel composed of 3.09% Co,
3.79% CH_4, and 50.70% CO_2 by volume, a flame temperature of approximately
870°C (1600°F) was maintained at the inlet to the heat exchanger with
about an 800°C drop across the 1.4 m (55 inch) length of the heat exchanger.
Based on these operating conditions and calorimetry measurements on the
cold side, the heat transfer coefficients were calculated and correlated
with an empirical relationship described by Jakob in reference (9). The
data point would also correlate with an extension of the Yagi and Wakao
correlation and is shown by point X in Figure 5. Two more test runs
for verification of this data are planned, in a lower Reynolds number range,
to establish which correlation is preferred. These runs will be completed in July.
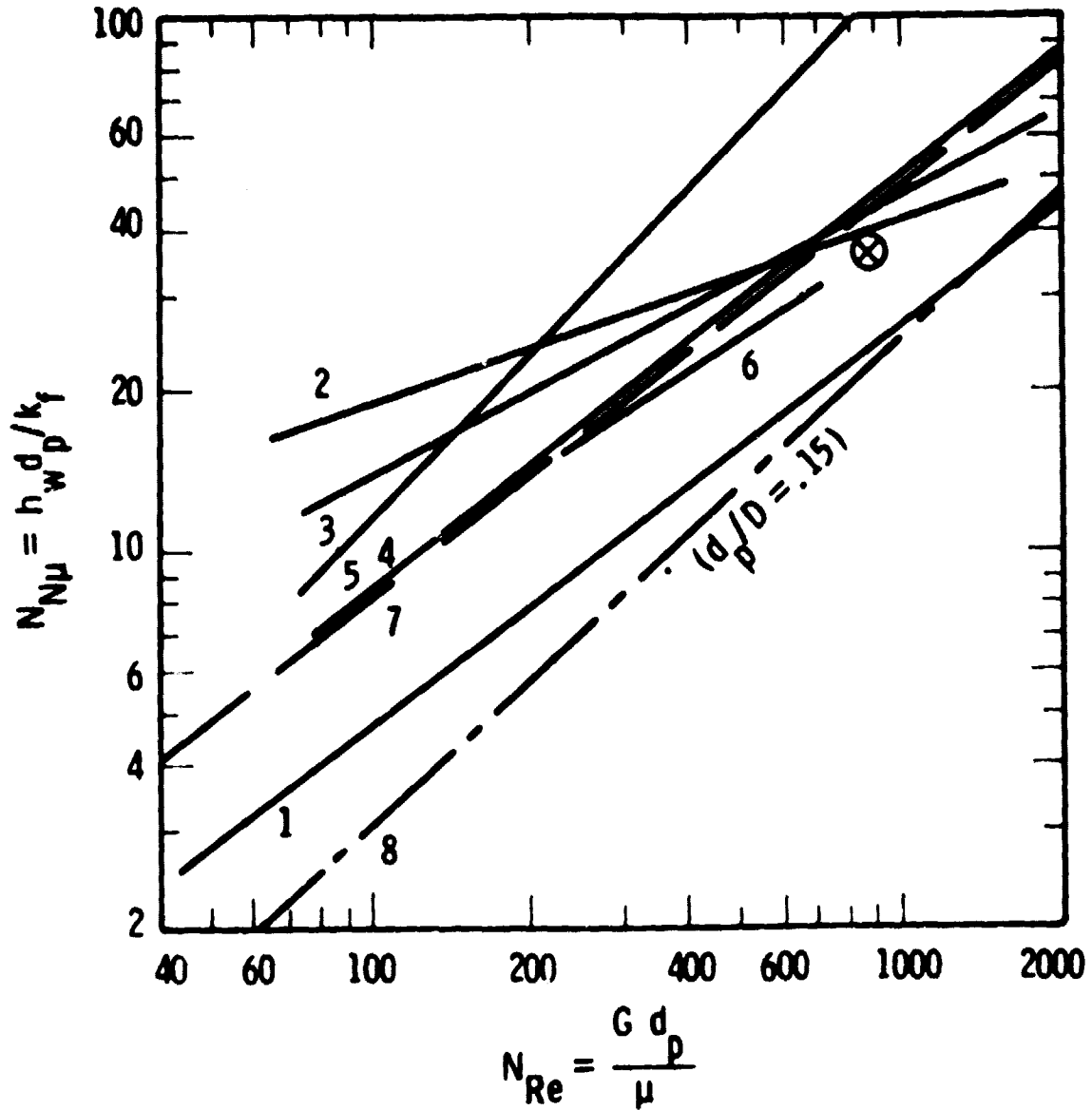
Figure 5 - Packed Bed Wall Heat Transfer Coefficients Curves:
(1) Aerov and Umnik; (2) Coberly and Marshall;
(3) Hanratty (cylinders); (4) Hanratty (spheres);
(5) Quinton and Storrow; (6) Yagi and Wakao;
(7) Thoenes and Kramer; (8) Leva

Dwg. 1715B31

Legend

⊗ Valve
Ⓣ Temp. Indicator
Ⓟ Pressure Gauge
⊕ Pressure Regulator
⊸⊢ Check Valve
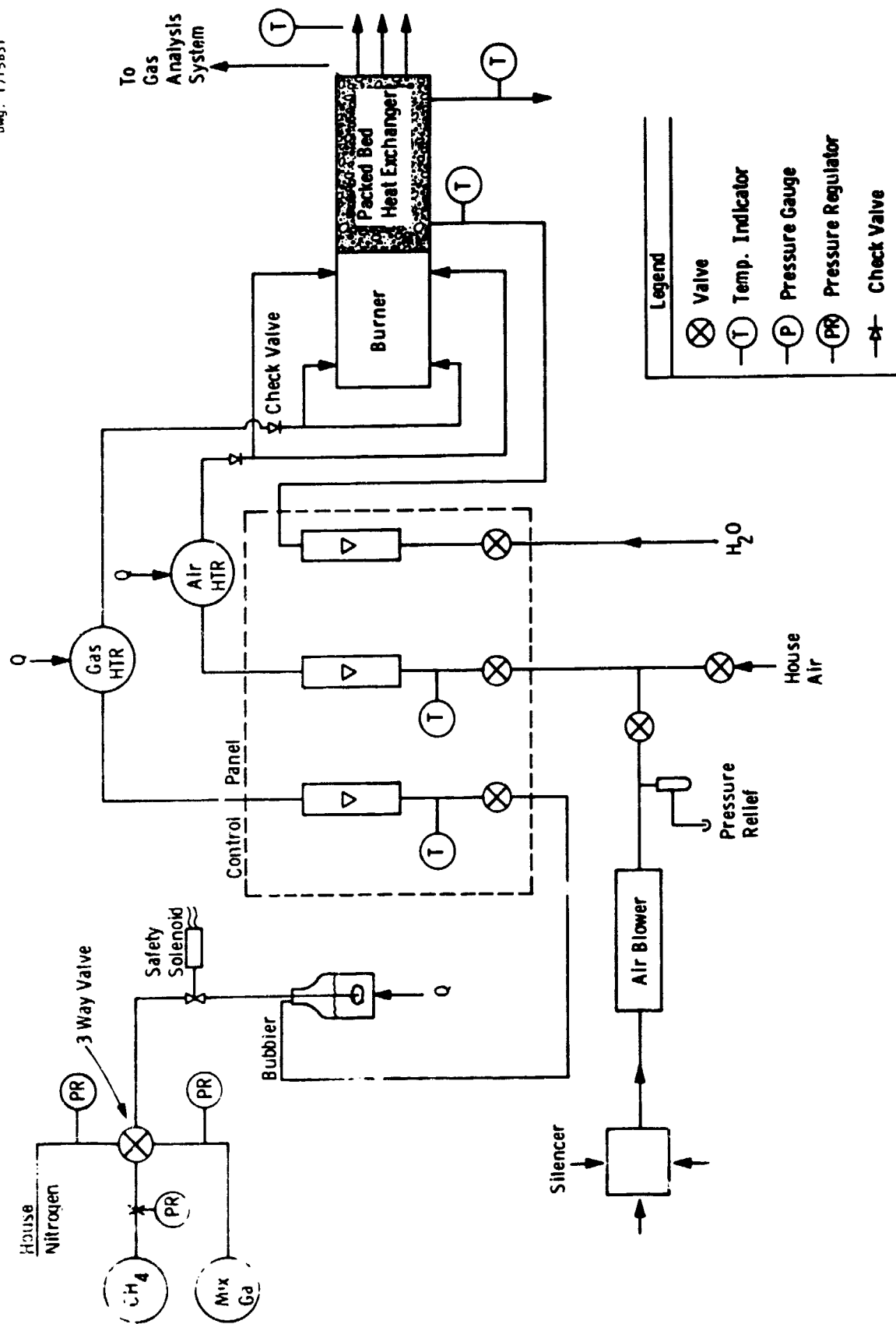
Figure 6 – Packed Bed Heat Exchanger Test Rig

Heat Exchangers

During this quarter efforts to obtain preliminary cost, configuration and technical design information for the 12 heat exchangers used in the fuel conditioner subsystem of the OS/IES continued. Several meetings were held with two potential suppliers, Heat Transfer Division of American Standard Co., Buffalo, NY and Harrison Radiator Division of General Motors Corp., Lockport, NY.

American Standard has provided preliminary costs, sketches and performance specifications for each of the heat exchangers. The designs are shell-and-tube types and coil types. Preliminary costs for the 12 heat exchangers are $38,546, with the Boiler, B-1, being the most expensive at $7820. The shell side (gas) pressure drop in B-1 was reduced during the evolution of the design to a value of 0.62 kPa (2.5 in H_2O). This has helped in reducing the overall parasitic energy loss in the fuel conditioner subsystem, since the high pressure drop made B-1 a major user.

Harrison Radiator has also furnished preliminary costs, sketches and performance specifications for the 12 heat exchangers. These designs utilize, as much as possible, the standard lines of Harrison Radiator. Exchangers E-1, -3, -4 are bar and plate gas/gas intercoolers conventionally used in aircraft applications. Exchangers E-5, -6, -7 and SH-1 usually serve as air-cooled lube oil coolers in aircraft applications. Exchangers B-1, C-1, CD-2 and CD-1 (w/o fins) are normally used as oil coolers in locomotives. They are round tube and fin types and have all mechanical construction. Heat exchanger C-2 is customarily used to condense Freon in an automotive air conditioner condenser. Preliminary costs for the 12 heat exchanger units are $12,110, with units B-1, C-1 and CD-2 being the most expensive at $2,475 each. In general, the Harrison costs are considerably lower than those of American Standard with the exceptions of units C-1 and CD-2. For unit E-1 Harrison requires 2 heat exchangers, but the total cost is still less than the comparable American Standard single unit.

Preliminary quotes and technical performance specifications
were obtained from Chromalox (Edwin L. Wiegand Div. - Emerson Electric Co.)
for the electric steam boiler (BP-1) and electric steam superheater (SH-2)
required from start-up to 1/3 power operation. Both of these units were
rated for 240 volts, single phase or 3-phase operation. Costs for these
units were as follows:

1. 12 kW electric steam boiler with an output of 16.5 kg/hr
   (36.2 lbs/hr) at 100°C (212°F), with a pressure ratio of
   0 - 689.4 kPa (0 - 100 psig)
   $2,389 less 15%

2. 2 kW circulation heater at 23.7 kW/m^2 (15.3 watts/sq. in.),
   Incoloy elements, sermetal coated body and flanges, with
   thermostat and high limit control
   $1312 less 15% (Add ~$400 for ASME Coding).

Other Ancillary Equipment

Information received from Otto H. York indicates that a 75 mm
Diam. (3 inch) section of their No. 241 demister with 150 mm deep (6 inch)
steel mesh packing should be adequate for removing water from steam
generated in B-1. The mesh has a nominal packing density of 0.2 g/cc
and will cost approximately $50.

Several revised quotations have been received for the gas
compressors and high pressure blowers. Because the overlapping of operating
conditions where each of these can be applied, there are wide variations
in costs for the same service duty. Quotations are being evaluated.

Considerable catalog and pamphlet literature has been collected
on pumps. This information is being reviewed for applicability.

4.6 10 kW Reformer

4.6.1 Test Station Construction

Construction of the 10 kW test station began in April and the
following work was completed this quarter:

27

- Construction of supporting structure and panel

- Installation of electrical supply lines and thermocouple connection lines

- Installation of temperature controllers, pressure gauges, flow meters, water pump and miscellaneous connecting tubing

- Installation of Mega-Pure Corning Still and its water supply line. This still will produce 12.5 ℓ/hr of pure water with a resistivity of 2.5 mega Ω - cm.

The following work is in progress and is expected to be completed in July:

- Construction of the water vaporizer and fuel gas preheater

- Installation of the control panel.

- Installation of automatic controls for the Corning Still.

4.6.2 Reformer Design

Following the conceptual design of a 10 kW reformer presented in the 6th Quarterly Report, the detail design of the reformer began this quarter and is near completion. Figures 7 and 8 show the top and the bottom sections of the reformer respectively. Some of the design details considered this quarter are:

a. Differential thermal expansion of the concentric tubes will be accommodated by a bellows as shown in Figure 7.

b. Reformer tube flange connections will be designed to facilitate disassembly.

c. Thermocouples and sampling tube locations will be guided by analyses using the BOLTAR computer program.

d. Packing spheres will be used for heat transfer enhancement

e. A burner-mixer made of a combination of castable and machinable ceramics will be incorporated to provide for admission and mixing of secondary air at low load operation.

28

FLANGE 1,
REFORMER

FLANGE 2,
REFORMER

FUEL IN

BELLOWS (2"I.D.)

FLANGE 3,
REFORMER

PRODUCT OUT

CATALYST
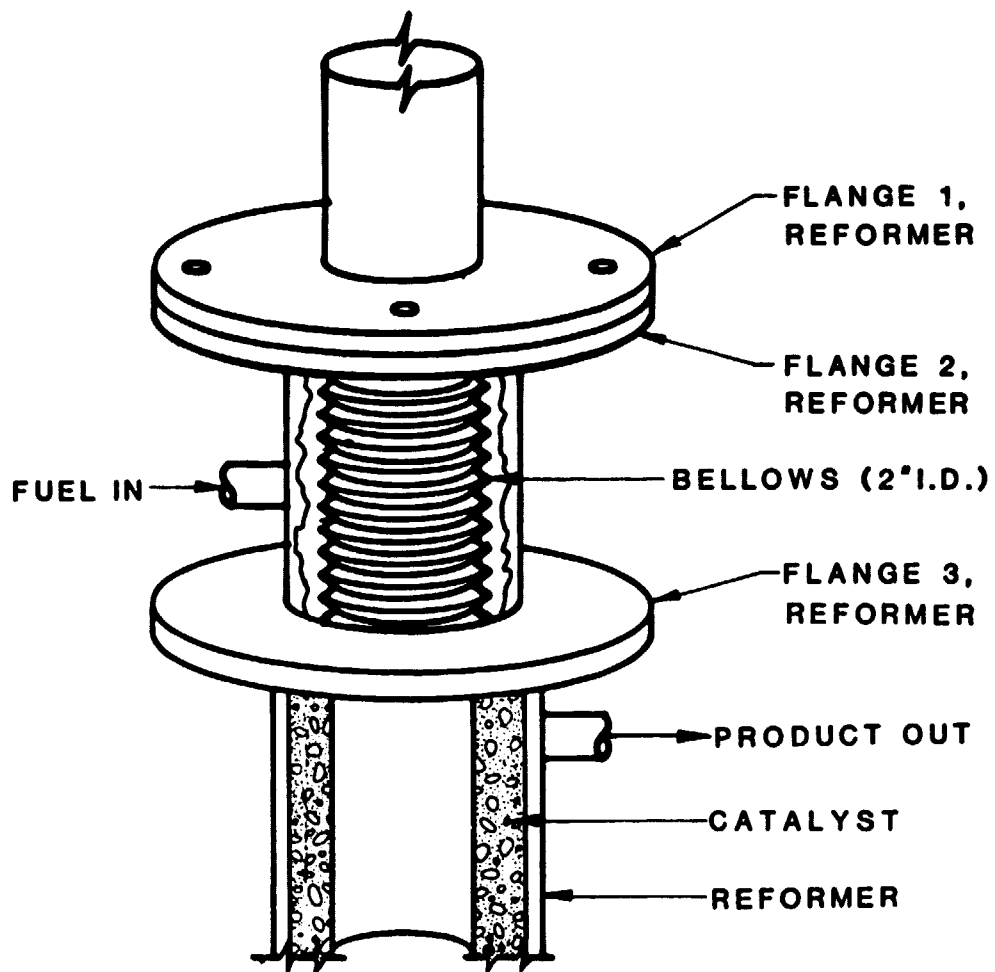
REFORMER

FIGURE 7 - TOP SECTION OF THE REFORMER
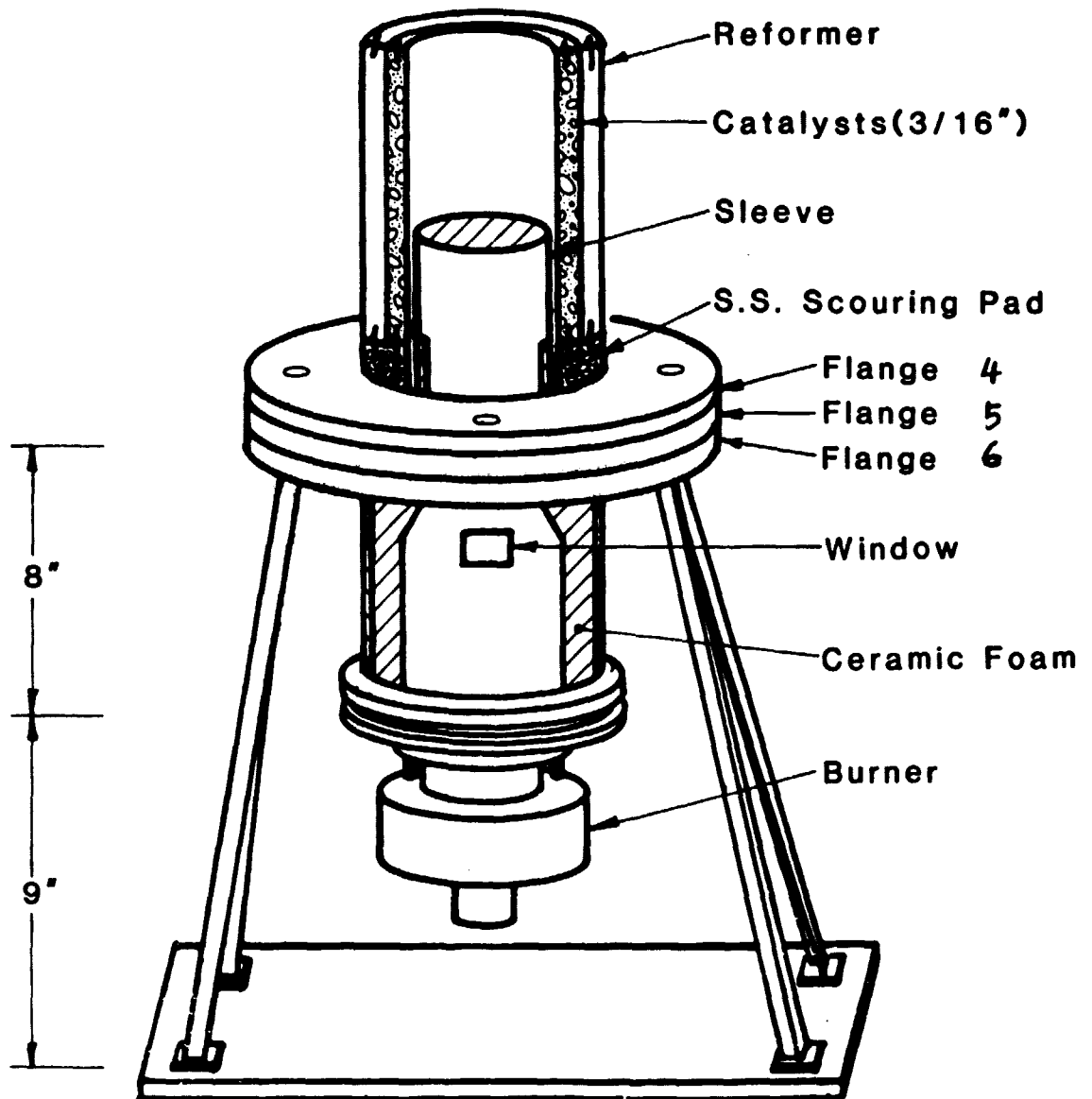
Figure 8 – BOTTOM SECTION OF REFORMER

4.6.3 Propane Burner

The preliminary test of the propane burner was completed this quarter. Various propane flow rates from 169.6 SLPH (6 SCFH) to 396.4 SLPH (14 SCFH), which is the full load requirement for a 10 kW reformer, were examined. The results were satisfactory. More tests will be performed to obtain the temperature profile with various air flow rates as soon as the burner mixer is completed.

An analysis of the effect of using propane, rather than spent fuel, on the heat transfer characteristics of the reformer was made.

The correlation for heat transfer in packed beds given by Jakob (reference 9)

$$\frac{h_c D_t}{K} = b \, D_t^{0.17} \left(\frac{D_p G}{\mu} \right)^{0.83} \left(\frac{C_p \mu}{K} \right)$$

was used to calculate the effect. The comparison was based on identical heat transfer rates and inlet and outlet temperatures for the two fuels. The effects of gas properties (viscosity, mass flow and specific heat) differences due to the fuel composition and the different fuel/air ratios were considered. For the reference case the calculated heat transfer coefficients on the combustion side differed by less than 15% (142 watts/m^2/°K for spent fuel vs. 123 for propane) for the two cases. The effect of this difference on the interpretation and applicability of the test results will be negligible.

4.6.4 Hardware Procurement

The Apple II computer and the Kaye ramp/scanner data logger have been received. The software calibration of the ram/scanner was ordered from Kaye Instruments, Inc. and has not been received yet. The delivery of the mass flow controllers has been delayed by two months and now is expected in the beginning of July.

---

(9) Heat Transfer, Vol. II, Jacob, M., John Wiley & Son, 1957

Vendors (including the Westinghouse R&D machine shop) were requested to bid on machining and welding of the reformer components. This work should begin in July and require about one month.

4.7 Prototype Conceptual Design

An effort was made to estimate the cost of manufacturing a reformer using the concept described in Westinghouse Disclosure Number AL 80-22 and discussed in the 4th Quarterly Report. It soon became clear that an accurate estimate of the cost could not be made until more details of the design were known (e.g. heat transfer augmentation scheme, reactor size, materials of construction) and these in turn cannot be decided until data from the 10 kW reformer and the spent fuel burner tests is collected and analyzed. However, some interesting questions and suggestions resulted from this effort and these are discussed below.

The OS/IES market comprises a large number of units and the anticipated sales exceed 6000 - 60 kW reformer modules per year. Furthermore, the relatively high operating temperatures of the reformer (600-1000°C) will probably require high nickel materials (such as Incoloy 800) which cost approximately $13/kg. Under these conditions the materials cost will be a significant portion of the manufactured cost and comparison among alternate designs can be reasonably based on materials cost only.

The above also leads to a consideration of ways to reduce the size of the reformer module. One way to achieve this is to carry out the relatively low temperature heat exchange between the streams (where very little reaction takes place) in a separate piece (or pieces) of equipment made of less costly material. An analysis of the external heat exchange requirements indicated that three exchangers would be required to replace the section in the integrated design. These exchangers could be made from conventional stainless steels and would probably be commercially available.

32

Another approach to reducing reformer cost is to design it
so that the material temperatures are reduced to levels that require less
expensive materials. This requires reducing the reaction temperature
levels or designing heat transfer surfaces so that the structural (wall
or tube) materials operate at temperatures close to the cooler gas stream.
Such design tradeoff studies require reaction rate data (which will be
obtained in the 10 kW reformer tests), heat transfer data (which will
be obtained in the burner tests) and a method for rapidly calculating
the effects of various conditions (which is being developed under
Subtask 4.8).

4.8 Computer Model

Work progressed smoothly on the computer model and several
parametric studies. The UTC 40 kW reformer and the ERC 10 kW test rig
design studies were completed. Catalyst particle size and heat transfer
effects were considered and more complete comparisons with experimental
data are being attempted. Future work will compare the model's pre-
dictions with the ERC 10 kW rig experimental results as they become
available.

The UTC 40 kW reformer studies were performed using the
available data and thermodynamic estimates of certain parameter values
(e.g. temperature, etc.). Use of the combustion gas model (with a
conservative correlation) predicts a low overall heat transfer coefficient
(22-45 w/m^2, °C). Adequate hydrogen production can be obtained, but
requires a high metal wall temperature (>1040°C). Arbitrarily increasing
the heat transfer coefficient above a value of 56 resulted in a failure
of the computer model to converge. The wall temperature profile model
eliminates one convergence loop. Consequently, it is operable over a
much wider range of input data. This model has predicted that inadequate
hydrogen production (<.75 $\frac{lb\ mol\ H_2}{hr}$) is obtained with the UTC design,
even with a reformate inlet temperature of 540°C, a parabolic temperature
profile starting at 590°C, and a heat transfer coefficient of 85 w/m^2,°C.
Uncertainties in the input parameters could be producing this effect.

The ERC 10 kW experimental reformer design has received extensive examination. The studies have concentrated on heat transfer, temperature, and catalyst particle size effects, using two wall profiles derived from UTC reformer information. Heat transfer affects the reformer's performance dramatically. Coefficients of 100-140 are required for a satisfactory hydrogen production rate. Changing the inlet reformer gas temperature over the range 260-540°C produced unexpectedly small variations in the exit conversion (<10%). However, the wall temperature profile choice causes large changes in the exit conversion, and essentially dictates the reformer's performance. This is to be expected.

Few actual heat transfer coefficient measurements exist for fuel cell reformers. An overall coefficient value of 28-56 has been "rumored," while accepted correlations give values that differ over a range of several hundred percent. The coefficients of 100-140 used with wall temperature profiles correspond to overall coefficients of approximately 50-70. Further uncertainty is contributed by the catalyst particle/ catalytic bed diameter ratio. The ratio should be in the .15-.2 range for the best heat transfer coefficient. Investigations with the existing correlations in the program show the present particle diameter (3.6 mm) to be close to the maximum (at 4 mm) for the ERC test rig dimensions.

Experimental information has been obtained from a smaller ERC reformer tube (46 cm long by 2.6 cm ID). Using appropriate input data, the model has produced predictions with similar temperature profiles. Endpoints are 10% low on conversion and 39°C high on exit temperature. This small reformer tube information will be investigated further and reported.

Work continues on upgrading the program's capabilities. Figures 9, 10 and 11 display 5 kW countercurrent flow, tubular geometry profiles drawn using the CALCOMP plotter option. Future work will center on obtaining solutions for the ERC 10 kW test rig design using combustion gas information, and comparing model predictions to the 10 kW rig experimental data as it becomes available.
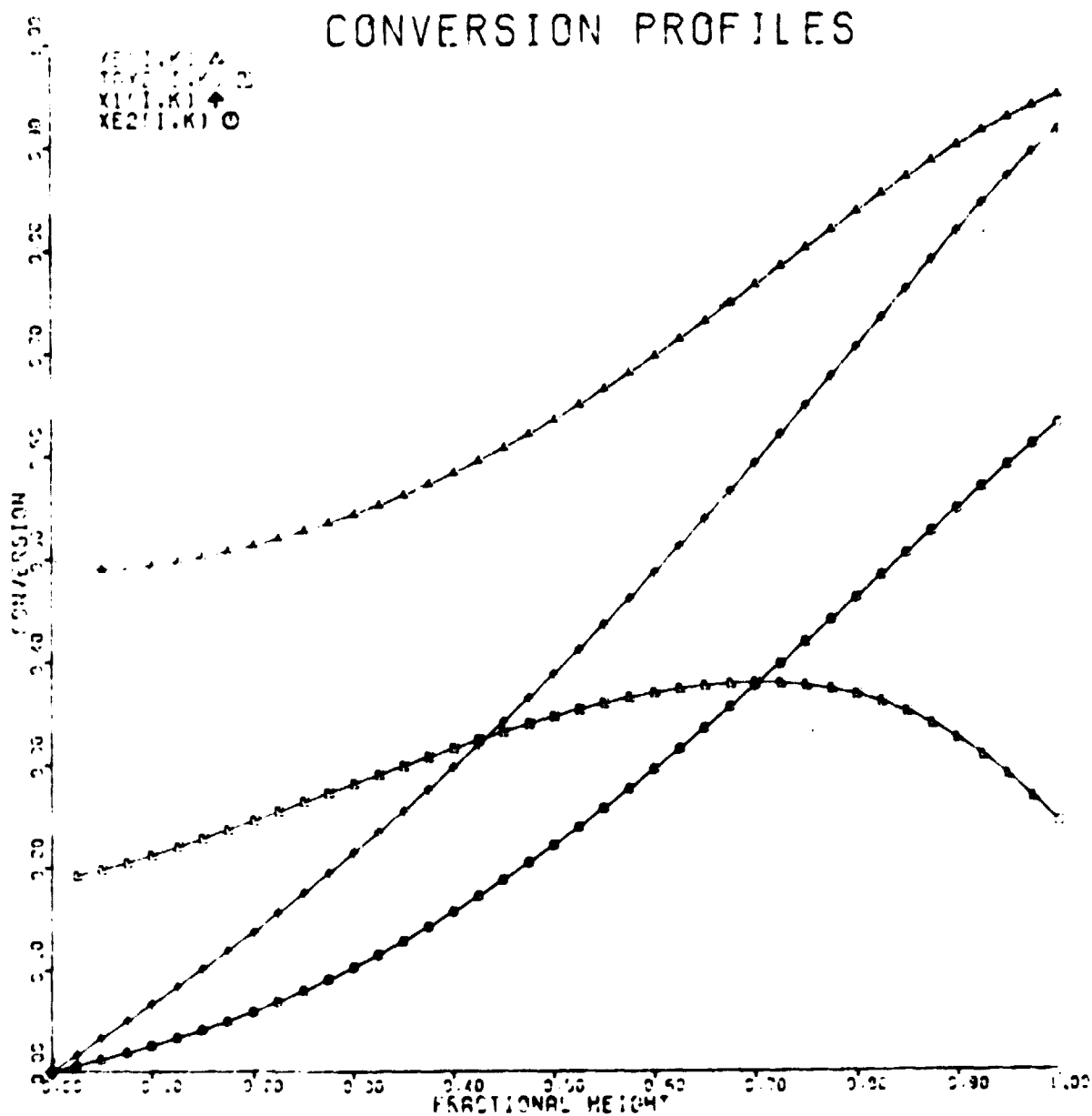
Figure 9 - 5 kW COUNTERCURRENT FLOW, TUBULAR
GEOMETRY CONVERSION PROFILES

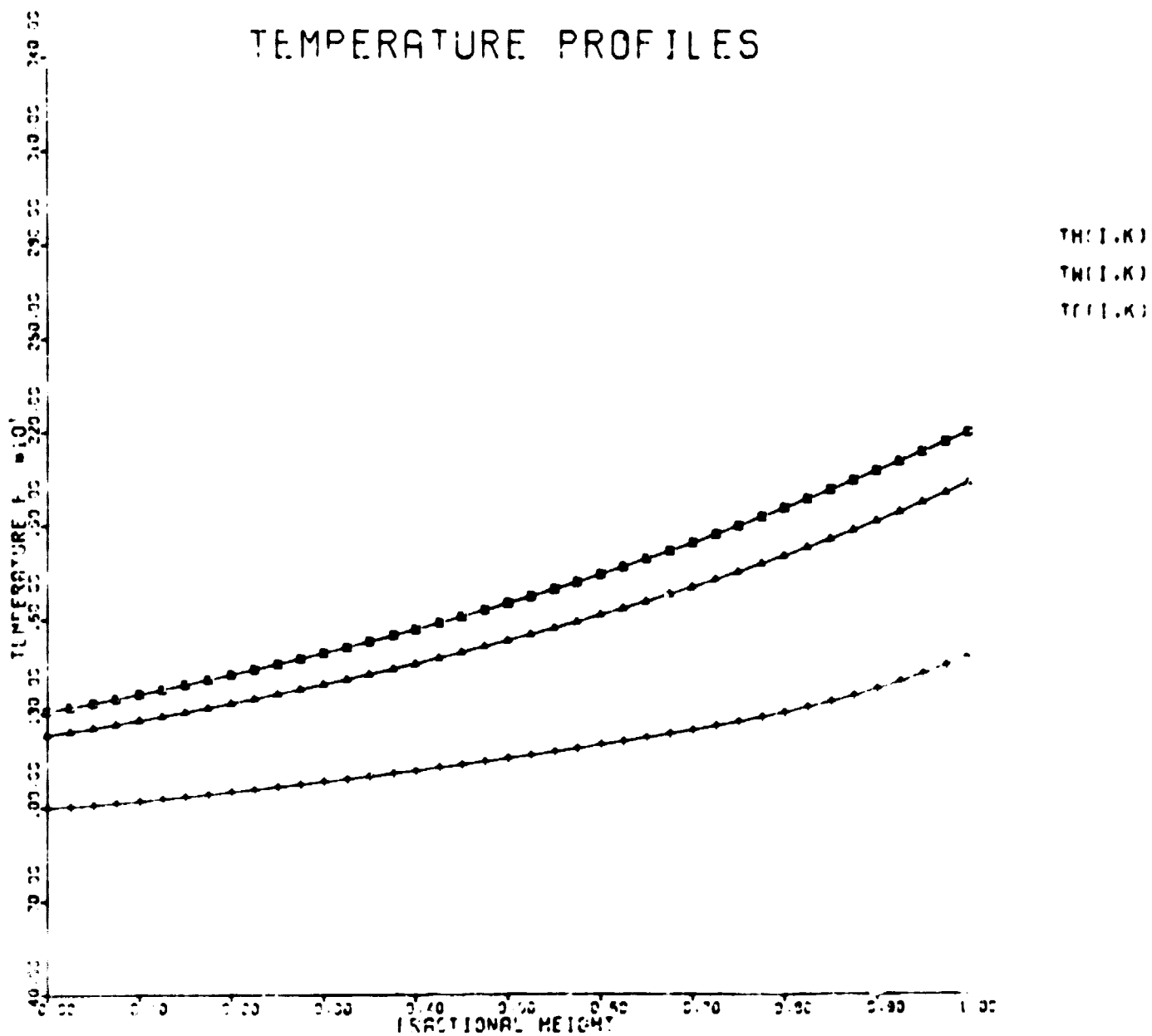Figure 10 - 5 kW COUNTERCURRENT FLOW, TUBULAR
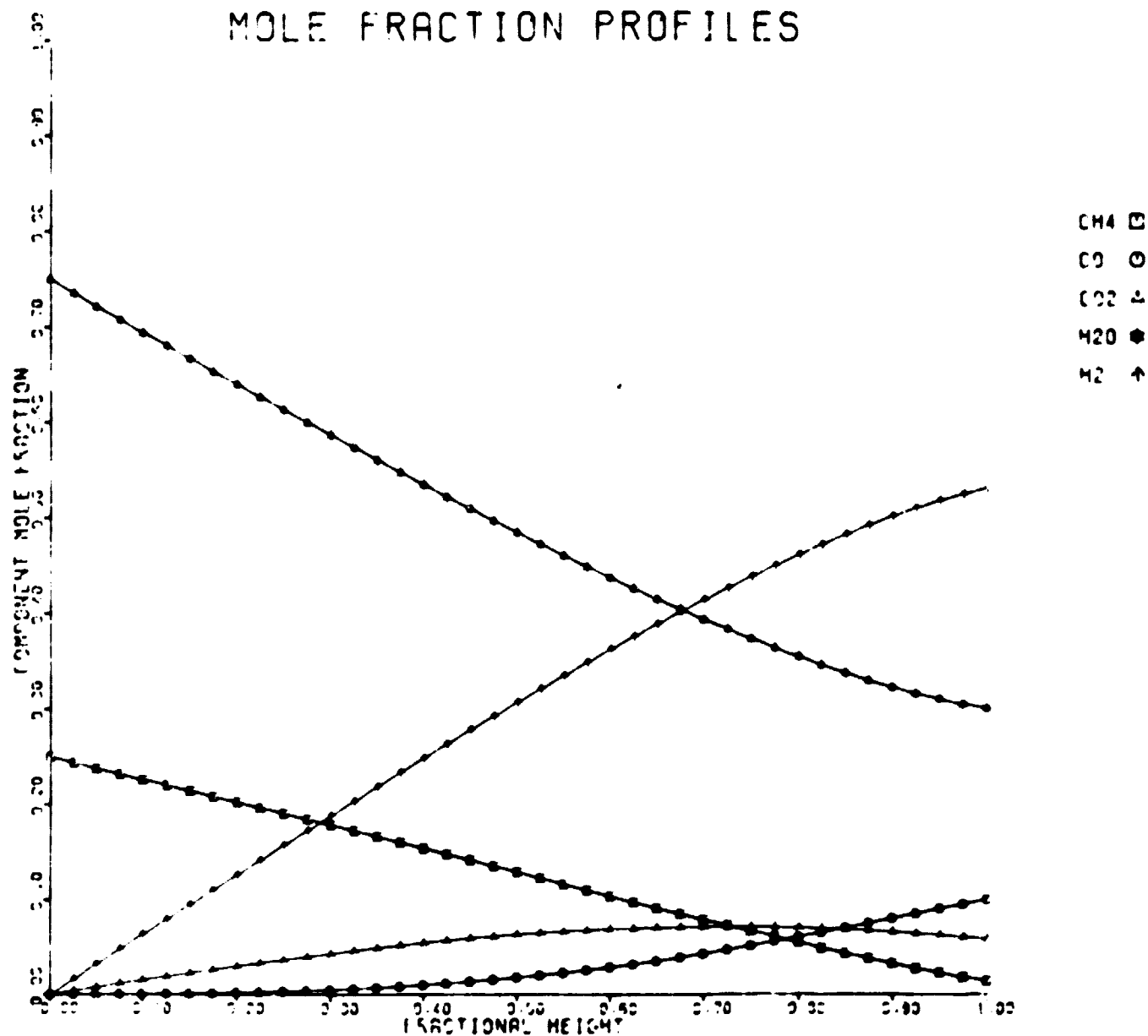GEOMETRY TEMPERATURE PROFILES

Figure 11 - 5 kW COUNTERCURRENT FLOW, TUBULAR
GEOMETRY MOLE FRACTION PROFILES

TASK 5: MANAGEMENT REPORTING AND DOCUMENTATION

5.1 Supervision and Coordination

Effective July 1, 1981, prime responsibility for this contract was transferred to Westinghouse Advanced Energy System Division (AESD). The Research and Development Center effort will continue as before under a part'al order transfer (POT) from AESD. The POT will include continuation of the ERC work under an R&D purchase order.

Coordination of the work on this project with the DEN3-201, DEN3-205 and the Westinghouse electric utility effort was continued.

5.2 Documentation and Reporting

The progress on phosphoric acid fuel cell and stack technology made under this project, DEN3-201, DEN3-205 and ERC and Westinghouse sponsored projects was described in a presentation at the 1981 National Fuel Cell Seminar.

The Sixth Quarterly Report and the April and May monthly technical narratives were submitted to and approved by NASA. They are now being prepared for distribution to the NASA supplied distribution. The January and February monthly technical narrative reports were distributed to the NASA supplied list.

The financial management reports(533M and 533P) for March, April and May were prepared and submitted to the NASA F: ject Manager along with supplementary cost and manhour graphs requested by the NASA Project Manager. The financial plan (533Q) for the Eighth Quarter was prepared and submitted to the NASA Project Manager.

Weekly and monthly technical highlights were reported to the NASA Project Manager.

III. PROBLEMS

None

IV. PLANS

TASK 1: DESIGN OF LARGE CELL STACKS

Stack 800 will be the first stack of more than 23 full size cells (1200 cm^2). The design must accommodate the increased creepage, voltage level and thermal expansion and contraction associated with the larger number of cells. The hardware concepts to achieve this accommodation will be reviewed by a team comprised of ERC, $\underline{W}$ R&D and $\underline{W}$ AESD personnel prior to submission to the NASA Project Manager for approval. To the extent possible these concepts will be incorporated in Stack 564 to experimentally verify their suitability.

TASK 2: STACK FABRICATION

The fabrication and assembly of Stack 564 will be completed in the next (eighth) quarter.

The fabrication of cell components and cooling plates for Stack 800 is underway and will be completed in the next quarter. The final assembly will take place during the first month (September) of the succeeding quarter.

TASK 3: STACK TESTING

Endurance testing of Stack 560 will continue.

Testing of Stack 562 has been completed and it will be disassembled in July. The disassembly will include close inspection of the cell components and stack hardware and the information gained will be used to guide the designs of Stack 564 and 800.

Pretesting and testing of Stack 564 will begin in the next quarter when its assembly is completed.

TASK 4: FUEL CONDITIONER DEVELOPMENT

Construction of the 10 kW reformer test station and fabrication of the reformer will be completed and testing will begin in the next quarter.

Several more tests of the packed bed heat exchanger at different gas flow rates, will be made and the results compared to the published correlation. The results will be used to select or develop an appropriate correlation for use in the BOLTAR computer program.

TASK 5: MANAGEMENT AND DOCUMENTATION

Coordination of efforts among the task leaders and between ERC and Westinghouse will be continued.

Technical review meetings will be held at the convenience of the NASA Project Manager and presentations to and meetings with DOE personnel will be scheduled as requested.

A design review meeting of Stack 800 is planned for the next quarter. Members of the NASA project team and the electric utility program will participate.

The task leaders' inputs to the Technical Status Reports will be edited and the reports will be submitted to the NASA Project Manager for patent approval. The management reports will also be prepared and submitted to the NASA Project Manager.